# Lab on a Chip

Accepted Manuscript




This is an *Accepted Manuscript*, which has been through the Royal Society of Chemistry peer review process and has been accepted for publication.

*Accepted Manuscripts* are published online shortly after acceptance, before technical editing, formatting and proof reading. Using this free service, authors can make their results available to the community, in citable form, before we publish the edited article. We will replace this *Accepted Manuscript* with the edited and formatted *Advance Article* as soon as it is available.

You can find more information about *Accepted Manuscripts* in the Information for Authors.

Please note that technical editing may introduce minor changes to the text and/or graphics, which may alter content. The journal's standard Terms & Conditions and the Ethical guidelines still apply. In no event shall the Royal Society of Chemistry be held responsible for any errors or omissions in this *Accepted Manuscript* or any consequences arising from the use of any information it contains.



ROYAL SOCIETY OF CHEMISTRY

www.rsc.org/loc

# Table of contents entry

Figure

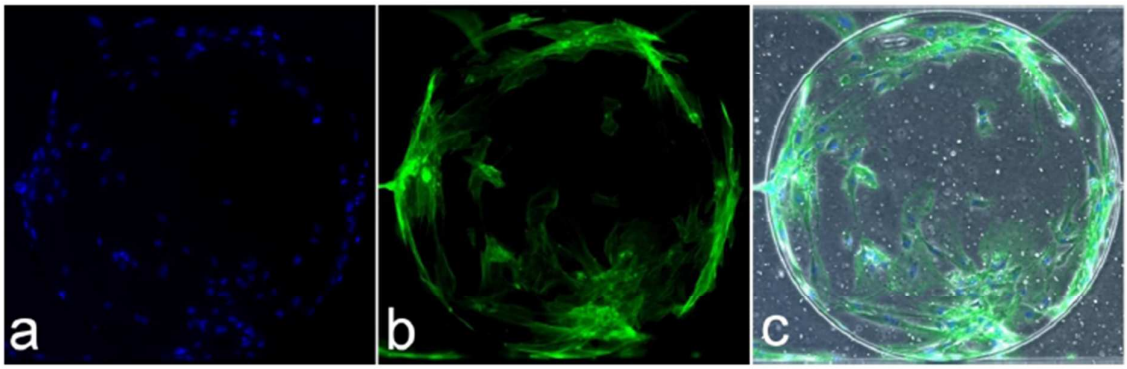


Text

In this paper, the design, development and validation of a novel high throughput microfluidic device enabling both the robust and rapid trapping of 100's to 1000's of single cells and their in situ clonal growth is described.

Lab on a Chip Accepted Manuscript

Journal Name

RSCPublishing

ARTICLE

# High-throughput, deterministic single cell trapping and long-term clonal cell culture in microfluidic devices

Cite this: DOI: 10.1039/x0xx00000x

Received 00th January 2012,
Accepted 00th January 2012

DOI: 10.1039/x0xx00000x

www.rsc.org/

Huaying Chen [a], Jane Sun [b], Ernst Wolvetang [b] and Justin Cooper-White [a, c, d, *]

We report the design and validation of a two-layered microfluidic device platform for single cell capture, culture and clonal expansion. Under manual injection of a cell suspension, deterministic trapping of hundreds to thousands of single cells (adherent and non-adherent) in a high throughput manner and at high trapping efficiency was achieved simply through the incorporation of a U-shaped hydrodynamic trap into the downstream wall of each micro-well. Post single cell trapping, we confirmed that these modified micro-wells permit the attachment, spreading and proliferation of the trapped single cells for multiple generations over extended periods of time (>7 days) under media perfusion. Due to its a) low cost, b) simplicity in fabrication and operation, c) high trapping efficiency, d) reliable and repeatable trapping mechanism, e) cell size selection and f) capability to provide perfused long-term culture and continuous time-lapse imaging, the microfluidic device developed and validated in this study is seen to have significant potential application in high-throughput single cell quality assessment and clonal analysis.

## Introduction

Single cell-level analysis techniques are increasingly being employed to better understand and provide new insights into the mechanisms controlling cell phenotype and fate choice and to assist in defining the quality measures of a range of cell types, including stem cells [1, 2]. These insights will be especially relevant to understanding the origins of heterogeneity in stem cells [3] and the nature (stochastic or deterministic?) of inducing pluripotency in somatic cells [4]. Studying single cell dynamics is however challenging and requires a) hundreds or thousands of isolated single cells to acquire statistically significant properties of the population [5], b) long-term clonal cell culture from single cell starting points, and c) continuous time-lapse imaging of cell growth and phenotype over multiple generations [6]. The application of traditional culture platforms (Petri dishes, well plates, etc.) to the analysis and long-term culture of high numbers of single cell starting points is however somewhat restricted. For example, single cells are often seeded into well plates by limiting dilution, but the number of cells in the wells is Poisson distributed [7], resulting in the number of single cells per well successfully acquired using this method being intrinsically limited. Using well plates with more wells (such as a 1536 well plate) may increase the number of single cells, but the single cell seeding process is still cumbersome and labour-intensive, without the investment in and assistance of a culture robot. Furthermore, due to difficulties in isolating shear sensitive single cells without suffering significant cell death when using alternate tools, such as Flow Assisted Cell Sorting (FACS), it is often difficult to ensure that the small number of single cells recovered post processing is truly representative of the population. During long-term cell culture, fresh culture media is required to regulate the pH level and supply the cells with necessary nutrients and growth factors [8-10]. Exchanging media in the well plate using pipettes during time-lapse imaging can however result in interruption of the imaging and hence loss of position and the ability to track cell behaviours [7].

A simple, microfabricated device designed for high-throughput, deterministic single cell trapping with a single manual injection of a cell suspension, and further, long-term cell culture under automatable media perfusion, and continuous time-lapse imaging would thus represent a novel, simple and inexpensive tool for researchers interested in studying single cell dynamics.

Microfluidic platforms have recently been widely employed for cell-based assays and long-term cell culture [7]. They have been used to manipulate single cells [11, 12], provide temporal and spatial control over the cellular microenvironment [13], enable

Lab on a Chip Accepted Manuscript

automated media perfusion [8, 10, 14], and study cellular responses to the external stimuli (e.g. shear stress [15], substrate elasticity [16], exogenous and paracrine factors [17], drugs [18]). Microwell-based devices have been developed for both short-term time-lapse imaging [19] and long-term cell culture for clonal/proliferation analysis [1, 20, 21], owing to their advantages in mechanical isolation of single/multiple cells and automatic media perfusion. However, in such device platforms, the cell seeding process is still largely based on the principle of limiting dilution (in microwells), which limits their repeatability and throughput in single cell analysis.

In response to the increasing demand for reliable and high-throughput single cell analysis, various mechanisms such as physical barriers and hydrodynamic traps have more recently been explored. For example, U-shaped microstructures on the bottom of a flow chamber were applied to trap, with high trapping efficiency, and culture single Hela cells for 24 hours [22]. Similarly, U-shaped hydrodynamic regions on the edge/wall of a microchannel [23, 24], or on the bottom of the flow chamber [25] have also demonstrated high single cell trapping efficiency. Microfluidic sieve-like traps have been fabricated on adhesive protein micropatterns to capture single cells and allow the growth of trapped single cells on the micropatterns [26]. Lin et al. [26] has recently summarised the single cell trapping efficiency of common trap designs, showing that there is significant variation between these designs (micropattern only (~40%) [27], microwells (40%-92.2%) [28], hydrodynamic sieve-live trap (55%-86.2%) [29] and hydrodynamic serpentine channel with side conduits (85%) [30]). These studies have provided substantive insight into the design rules for high efficiency single cell trapping, however none of them are capable of long-term single cell culture/clonal analysis, since either the cell culture area is too small for cell progeny or the cells are exposed to larger shear stress during media perfusion.

Herein, we report the design and optimization, aided by computational fluid dynamics and experimental validation, of a two-layered microfluidic platform for single cell capture and subsequent culture and clonal expansion of both adherent and non-adherent cells. The simplicity of this device design concept allows for the future integration of other microfluidic components upstream of the capture and culture region, for example, a resistive flow network for factorial provision of bioactive factors [17, 31], to enable one to study single cells, including stem cells, in a precisely controlled microenvironment (such as the concentration of growth factors, small molecules and fluid shear stress).

## Materials and Method

### Computational Fluid Dynamic (CFD) assisted design and analysis

The design concepts for the herein described microfluidic single cell capture and culture devices were firstly modelled to achieve optimised device geometry prior to fabrication and experimental validation (see Section S1 in Supplementary Materials). To evaluate the influence of device geometry (well depth / channel height = 5, 1 and 0.5), cell size and media flow rate on the single cell retention inside the U-shaped trap, four single-well models (see Table S1 for the detailed dimensions in Supplementary Materials), with a fixed cell in the trap were created using Ansys ICEM CFD 14.0 (Ansys®) and assessed using Ansys CFX 14.0 (Ansys®). The single-well model (see Figure S1a) consisted of a 1.06 mm wide channel on top of a well (1-mm in diameter), a 27-μm wide U-shaped trap, a 10-μm wide channel and a sphere (representing a cell, either 14 μm or 24 μm in diameter) fixed on the floor of the trap. The device Reynolds number is given by

$$Re = \frac{2\rho q}{\mu(w+h)} \quad (1)$$

, where $\rho = 1000$ kg/m$^3$ and $\mu = 7.987 \times 10^{-4}$ Pa·s are the density and viscosity of the cell culture media at 37 degrees Celsius, $w$ and $h$ are the width and the height of the channel and $q$ is the flow rate of the media. The Reynolds numbers studied in all models were 0.0005, 0.005, 0.0124, 0.0248, 0.0496 and 1.8. All boundaries except inlet and outlet were set as non-slip walls. To determine the critical Re for lifting the cell out of the trap in model 50-50, Reynolds numbers of 10, 11, 12, 15, and 20 were studied. A large cell with the diameter of 24 μm (referred to as model 50-50L) was employed to study a) the influence of the cell size on the fluid induced forces on the cell and b) if a larger cell could still be retained in the trap (Figure S1c). The full-hex mesh was employed for all models (Figure S1 b and c). Details of the outcomes of the CFD investigation and associated mechanical equilibrium analysis and micro Particle Imaging Velocimetry (μPIV) validation of the CFD outputs are included in the Supplementary Materials.

### Device design

Post CFD analysis and optimisation, two types of devices with the same single cell trapping mechanism were designed for the single cell capture and long-term culture of both adherent (referred to as Design A, see Figure 1a) and non-adherent cells (referred to as Design B, see Figure 1b). Both designs consist of two layers (see Figure 1c): a glass slide top layer and a PDMS bottom layer with either a serpentine flow channel (either 1 mm or 0.5 mm wide) and 528 (for 1 mm-wide channel) or 1888 (for 0.5 mm wide channel) wells underneath the flow channel, or a tree-pattern channel and 1888 wells underneath the flow channel. Both the flow channel and the wells are 50 μm deep (see Figure 1c). The well diameter is either 1 mm or 0.5 mm for Design A and 0.5 mm for Design B. They are spaced at 50 μm in the flow direction. In both designs, there is a notched, U-shaped trap on the downstream edge of each well with a 10-μm wide microchannel connecting to the downstream well (see Figure 1c). This microchannel is designed to generate a precisely regulated hydrodynamic trap to retain single cells, even when there is flow through the serpentine/tree-pattern flow channel. The wells have also been designed to have large surface area to provide enough space for the spreading and

Lab on a Chip Accepted Manuscript

 This journal is © The Royal Society of Chemistry 2012

proliferation of the trapped single cells and their progeny over multiple generations. This is especially important for the long-term culture of adherent cells whose surface area is much larger than that of the non-adherent cells. The media in Design A, with 0.5 mm channel and wells, flows through the single serpentine channel. However, the media injected into the inlet of Design B at the same flow rate is split into 32 × 0.5 mm wide channels. Therefore, the shear stress [32] on the trapped cells in Design B is only 1/32 of that in the Design A, when the inlet flow rate is the same. This significant decrease in the shear stress prevents the flushing out of the trapped single non-adherent cells and their progeny during media perfusion in long-term culture.

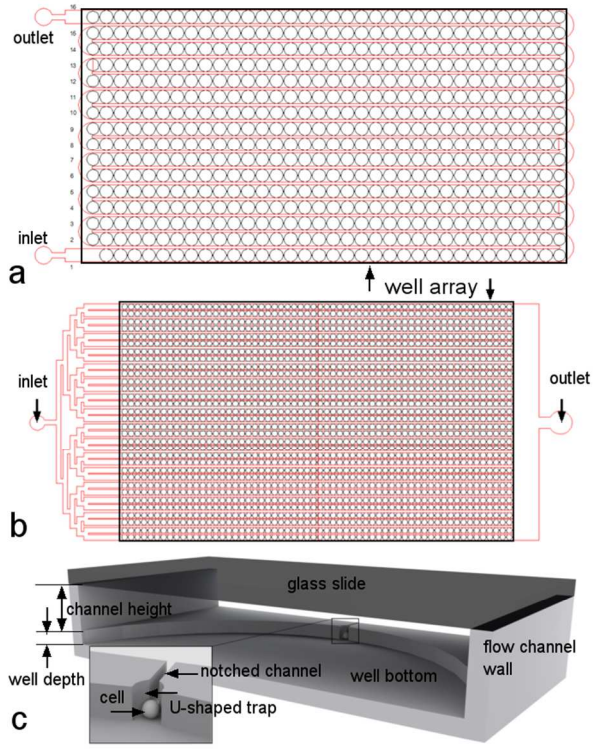


Figure 1. a) Design A (for trapping and culture of adherent cells) with 588 x 1 mm diameter wells and a serpentine channel on top of wells. b) Design B (for the trapping and culture of non-adherent cells) with 1888 x 0.5 mm diameter wells and a tree-pattern flow channel. c) Cross section of one well for both Design A and B. The bottom is a PDMS layer with the well and the microchannel. The top layer is a glass slide. The notched channel connects two adjacent wells through the U-shaped single cell trap.

### Device fabrication

All devices were fabricated by soft lithography which has been described elsewhere [21, 31]. Briefly, following the dehydration of the silicon wafer at 200 °C for 30 min, PerMX™ 3050 photodielectric dry film (DuPont™) with the thickness of 50 µm was laminated on the wafer at 80 °C with the roll speed of the 1 m/min using a laminator (Albyco PHOTOPRO 33). The film was soft baked at 95 °C for 10 min, and thereafter exposed to UV light under a mask with the serpentine / tree-pattern flow channel (see Figure 1 a and b) with the exposure dose of 500 mJ/cm$^2$. The film was further baked for 5 min until the serpentine flow channel and the alignment mark appeared, and then another piece of PerMX™ 3050 dry film was laminated on the first layer, before it was exposed to UV light under a mask with the individual wells (see Figure 1). Following 5-min baking, both layers were developed in propylene glycol monomethyl ether acetate (PGMEA) (Cat No. 484431, SIGMA-ALDIRCH) for 20 min. Finally, the mould was washed using DI water and dried using compressed nitrogen.

Sylgard® 184 elastomer base and curing agent (Dow Corning® Corporation, Midland, USA) were evenly mixed at a weight ratio of 10:1 and completely degassed under vacuum. The polydimethylsiloxane (PDMS) mixture was cast against the mould of the well array, before being degassed again for 20 min. Afterwards, the PDMS mixture on the mould was baked in an oven at 60 °C overnight. The cured PDMS replica was peeled off from the mould. The inlet and outlet ports were punched using a Harris Uni-core™ cutting tip (Ø 0.75 mm). Both the replica of the mini-well array and a glass slide (76 × 26 mm) were then treated using oxygen plasma for 30 sec, before they were brought into conformal contact. The bonded device was then connected to polyethylene tubing (Cat No. 427411, BD) using 21-gauge flat-ended needles.

### Single microsphere trapping

To validate and characterise the trapping efficiency of the three different devices listed in Table 1, Polybead® microspheres with the diameters of 6, 15, 20 and 25 µm (i.e. ranging from smaller to larger than the trap size) were utilized. The microsphere suspension was diluted into 125 000 microspheres/mL and manually injected into each device (one size at each time). Following microsphere loading, DI water was injected into the device at various flow rates (referred as flushing flow rates), ranging from 0.25 µL/min to 45 µL/min to displace excessive microspheres out of the wells / traps. A minimum of 350 traps, in each device, was imaged at every flow rate using the microscope with a motorized X-Y-Z stage.

Table 1. The parameters of three devices applied in the single microsphere trapping study.

| Device ID | Dimension (mm) | Well diameter (mm) | Channel height and well depth (µm) | Notch channel width (µm) | Trap width (µm) | Number of wells | Volume (µL) per unit (well and the top channel) | Total inner volume (µL) |
|---|---|---|---|---|---|---|---|---|
| 1-27 | 40 × 19 | 1 | 50 | 10 | 27 | 528 | 0.09 | 51 |
| 1-18 | | | | | 18 | | | |
| 0.5-27 | 40 × 22 | 0.5 | | | 27 | 1888 | 0.02 | 48 |

Lab on a Chip Accepted Manuscript

**Cell culture and cell cycle synchronisation**

Human dermal fibroblasts (HDFs, CRL-2429) were cultured in T75 flasks in an incubator at 37 °C and 95% humidity using Dulbecco's Modified Eagle Medium (DMEM) supplemented with 10% fetal bovine serum (FBS) and 1% penicillin-streptomycin (P-S). When 95% confluent, the cells were trypsinized using TrypLE and resuspended into DMEM (without FBS and P-S) to achieve a concentration of 500 000 cells/mL. This cell suspension was applied for the single cell trapping and culture study.

K562 cells, a human immortalised myelogenous leukemia line, were cultured in a T25 flasks with RPMI 1640 (61870-036, Life Technologies, Australia) supplemented with 10% FBS and 1% P-S. Before being loaded into the microdevice, the K562 cells were resuspended into the culture media with the concentration of 500 000 cells/mL.

To assess the impact of cell cycle status on single cell growth, HDFs were used as cultured ('non-synchronised') and also post cell cycle synchronisation. HDFs are able to be synchronised to G0/G1 phase by serum starvation [33]. Briefly, cells cultured to 50% confluence in a T75 flask with DMEM (+10% FBS and 1% P-S) were washed three times using phosphate buffered saline (PBS), fed with low-serum synchronization medium (DMEM + 0.5% FBS and 1% P-S) and incubated for 26 hours. Cells were then trysinized and washed twice using PBS, before being resuspended into 0.5 ml ice cold PBS. Afterwards, 2 mL ice cold 70% ethanol was added to fix the suspended cells. After two-hour refrigeration, the cells were washed using PBS for three times and incubated in 0.5 mL propidium iodide / RNase A staining buffer (926769, invitogen) at room temperature for 30 min. The stained cells were thoroughly washed using PBS and resuspended into 2 mL PBS (the final concentration is approximately 1.5 million cells/mL). Finally, a flow cytometer (accuri™, BD) was employed to determine the proportion of cells in G0/G1 and G2/M phases.

**Single cell trapping and culturing of HDFs**

**NON-SYNCHRONISED HDFS**

The Device '1-27' (see Table 1) was placed inside a microfluidic enclosure (see Figure S4 in Supplementary Materials), which was mounted on the motorized stage of a time-lapse microscope (IX81, Olympus®) with a temperature and humidity controlled enclosure to maintain the temperature at 37 °C. 5% $CO_2$ in air was continuously injected into the microfluidic enclosure. 70% ethanol was injected into the device at 15 µL/min for 40 min to sterilise the device, before phosphate buffered saline (PBS) was applied to rinse the device at the same flow rate for 20 min. Prior to the introduction of cells, a solution of 0.8% bovine serum albumin (BSA) was injected at 15 µL/min for 1 hour to coat the PDMS surface, before the device was flushed using PBS. In the absence of a pre-coating of BSA, HDFs would adhere non-specifically to the PDMS surface within the wells during capture and not just in the traps, which results in the adhesion of multiple cells in each well. However, when the PDMS was coated with BSA, the HDFs were not able to attach on the substrate without the aid of adhesive proteins (such as fibronectin, Matrigel, etc.). 0.2-0.3mL HDF cell suspension in DMEM (without FBS and P-S) with the concentration of 500 000 cells/ml was thereafter manually injected into the device for 1 min to capture the cells, before DMEM with 30% FBS, 2% P-S and 50 µg/mL fibronectin was immediately injected into the device at the flow rate of 0.5 µL/min (Re=0.02) to displace excessive cells. Fibronectin was added to the culture media during this stage in order to coat the well bottoms with an adhesive protein to encourage cell attachment and growth post capture. After 10-min of injection, the 350 traps were imaged to check the single cell trapping efficiency. After imaging, the device was kept on the microscope stage for continuous time-lapse imaging. 23 wells (1 or 2 wells per row along the serpentine channel) initially seeded with single cells were imaged every 10 min for 9 days. The device with the perfusion system was moved into an incubator from Day 9 and cells were continuously cultured till day 14. DMEM with 30% FBS and 2% P-S in a 3 mL syringe (Terumo®) was perfused into the device at the flow rate of 0.4 µL/min to provide the cells with nutrients. The syringe with media was replaced with a new one containing fresh media every 3 days.

On day 14, cells cultured in the microdevice were fixed *in situ* using 4% formalin and stained using Hoechst 33342 (staining nuclei) and Phaloidin Alexa Fluor 488 (staining actin filaments). Both phase contrast and fluorescent images of stained cells in 50 randomly selected wells were taken using the time-lapse microscope. Each experiment was repeated a minimum of three times (three technical replicates).

**SYNCHRONISED HDFS**

To understand if any observed heterogeneity of single cell growth is dominated by the cycle status of cells when they were loaded into the device, the HDFs were synchronised to G0/G1 phases using serum starvation. After being cultured in low-serum synchronisation medium (DMEM + 0.5% FBS and 1% P-S) for 26 hours, 89.3% cells were synchronised to G0/G1 (see Figure S5 in Supplementary Materials). These synchronised cells were further cultured in either well plates or the Device '1-27' from the single cell starting point to study the cell growth heterogeneity. The synchronised HDFs were trapped as single cells (using the same protocol as described above) in Device '1-27'. Then DMEM (supplemented with 30% FBS and 2% P-S) was injected into the device at the flow rate of 0.4 µL/min. 77 single cells (four or five cells per row along the serpentine channel) were randomly selected for continuous time-lapse imaging every 10 min for seven days. The media in the syringe was refreshed every two days. Each experiment was repeated a minimum of three times (three technical replicates).

**Single non-adherent cell (K562) trapping and culture**

Single K562 cells were trapped and cultured in the tree-pattern device (Design B with 0.5 mm well and 27 µm wide trap, see Figure 1b) to demonstrate the ability of this device in non-

Lab on a Chip Accepted Manuscript

 This journal is © The Royal Society of Chemistry 2012

adherent cell culturing with media perfusion and continuous time-lapse imaging for clonal analysis. Following the sterilization of the tree-pattern device, 0.2-0.3 mL of non-adherent K562 cell suspension (500 000 cells/mL) was manually injected into the tree-pattern channel device for 1 min. Then RPMI 1640 (61870-036, Life Technologies, Australia) supplemented with 30% FBS and 1% P-S was contained in a 3 mL syringe and injected into the device at the flow rate of 15 μL for 10 min to flush the excessive cells and deposit single cells in the traps. Afterwards, the media flow rate was reduced to 0.2 μL/min to perfuse the cells for one week. 88 wells (2 or 3 wells per row of the tree-pattern channel, see Figure 1b) were selected to image using a 10× objective every 5 min for the whole culture period. Each experiment was repeated a minimum of three times (three technical replicates).

### Image analysis

Matlab code (MATLAB R2013) was developed to segment spheres / cells in the images from the single microsphere/cell trapping experiment (see Section S4 in Supplementary Material for the segmentation of the microsphere). The segmentation accuracy of this code is greater than 96%. The time-to-first-division of all imaged cells and growth curves of selected cells were obtained by analyzing the image stacks. The image stacks recording the movement and division of both HDFs and K562 cells were employed to study the cell growth dynamics. Four individual clones (two clones from each cell type) were semi-manually tracked with the aid of the Matlab code [21].

## Results

### Single microsphere trapping

The single sphere trapping efficiency (SSTE) refers to the percentage of wells trapping single microspheres. It is the ratio of the number of wells with single microspheres to the total number of wells. Figure 2a shows the micrograph of 25-μm microspheres trapped in the Device '0.5-27' when the flushing Re is 0.6 (see Supplementary Video 1 for this process). When injected into all devices, 6 μm microspheres were able to either flow through the notch channel (10 micron wide) at low flow rates or lift up at the downstream edge and flow into the next wells at high flow rates (see Supplementary Video 2). No 6 μm microspheres were trapped in any of the three device designs.

The SSTE of 15, 20 and 25 μm microspheres in three devices under various Re numbers is shown in Figure 2b-d. It can be concluded from Figure 2 that all devices are able to trap single microspheres with high efficiency within a large Re range. The max SSTE for Devices '1-27', '0.5-27' and '1-18' is 98.5% (for 20 μm microspheres), 98.2% (for 25 μm microspheres) and 97.5% (for 15 μm microspheres), respectively. For Device '1-27', the SSTE of 20 and 25 μm microspheres stays higher than 95% when Re<1.4. As the Re increases further to 1.8, the SSTE of 25 μm microspheres dramatically dropped to 75.7%, while SSTE of 20 μm microspheres remains stable. The SSTE of the 15 μm microspheres increases from 88.7% to 93.9% as the Re rises from 0.2 to 1.4. In Device '0.5-27', the SSTE of 20 and 25 μm microspheres was similar to that in Device '1-27'. However, when Re increases further from 1.4 to 2.8, the SSTE drops to 94% and 89.2% for the 20 and 25 μm microspheres, respectively. The SSTE of the 15 μm microspheres continues increasing from 63.9% to 80.5% as the Re rises from 0.2 to 2.8. For Device '1-18', the SSTE of 15 μm microspheres is constantly larger than 95% when 0.6<Re<1.4, while the SSTE of 20 and 25 μm microspheres is inversely correlated to Re. As Re rises from 0.02 to 1.4, the SSTE of 20 μm microspheres gradually decreased from 60.4% to 45%, while a dramatic drop of SSTE of 25 μm microspheres from 72.5% to 11.6% is found when Re increased from 0.02 to 0.2.

Lab on a Chip Accepted Manuscript

Journal Name RSCPublishing

ARTICLE

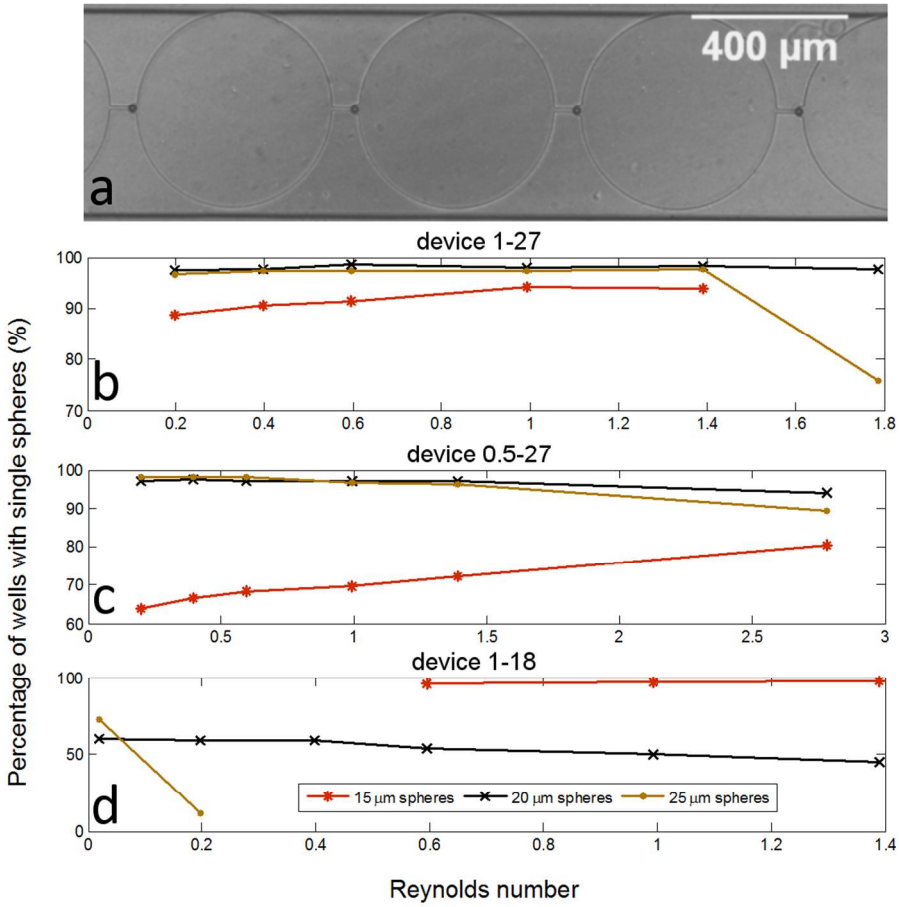


Figure 2. a) A micrograph of 25-µm microspheres trapped in the Device '0.5-27' when Re=0.6. b-d) The percentage of wells trapping single microspheres at various Re values. The microspheres with the diameters of 15, 20 and 25 µm were manually injected into three devices, before DI water was injected into each device at various flow rates to flush the excessive cells out of the wells. The microspheres retained in 350 traps in each device under various Res were imaged at each Re. No 6-µm microspheres were trapped.

The SSTE for all devices are related to both the size of the microspheres and the flushing flow rate. The devices reported in this study are able to select the microspheres (and cells, as shown later) of a targeted size by adjusting the width of the single cell trap and the flushing flow rate. Microspheres with the diameter slightly smaller than the trap width were able to be trapped at high efficiency, regardless of the diameter of the well, such as the 20 and 25 µm microspheres in 27-µm wide traps and 15 µm microspheres in 18-µm wide traps. However, when the sphere diameter (15 µm) is much smaller than the width of the trap (27 µm), there is an increasing number of wells with multiple spheres in the same trap, which reduces the SSTE. The SSTE could be raised by increasing the flush flow rate (Figure 2 b and c). For microspheres larger than the width of the trap (Figure 2 d), the SSTE is lower than 72% and inversely correlated to Re.

**Single cell trapping and long term culturing of HDFs**

The number of non-synchronised HDF cells trapped in each individual trap of 350 wells in the Device '1-27' was counted to confirm the ability of this device for high-throughput deterministic single cell trapping. After manual injection of the 0.2-0.3 mL cell suspension (500,000 cells/mL) for 1 min, even though single cells are lodged within the trap, multiple cells may end up sediment into each well from the bulk media. Media was thus injected into the device at the flow rate of 0.5 µL/min (Re=0.02) post this seeding step to flush the excess cells out of the device and the wells. After this flushing process, the majority of the wells were loaded with single cells (see

Lab on a Chip Accepted Manuscript

Figure 3a). The single cell trapping efficiency in this set-up was 78.9% ± 3.7% (N=350, see Figure 3b). There were 16.8% and 4.2% wells trapping 0 and 2 cells, respectively. The mean diameter of HDFs in suspension in this experiment was measured to be 24.3 µm.

Post coating the surfaces of the culture chambers with fibronectin (see Section 'Non-synchronised HDFs' in Materials and methods), the trapped non-synchronised single cells were cultured in situ with media perfusion and continuous time-lapse imaging for 9 days, before being moved to an incubator and continuously cultured until day 14. Please refer to Supplementary Video 3 for the proliferation of the single HDF cell shown in Figure 3a in 206 hours. From this study of long-term single HDF culture, it was clear that: a) the division rate of cells varied significantly - for example, some individual cells post capture did not divide in the 14-day culture period, whilst others showed significant growth, for example, one of the single cells proliferated into 123 cells in 14 days (see Figure S8 in the Supplementary Materials); b) cells preferred to grow along the well wall if there was enough space; c) the size of the well was large enough for extended, two week long culture of HDFs starting from single cells; d) in some cases, there were small numbers of cells growing on the ceiling (glass plate) of the flow channel instead of the PDMS well floor.

Single cell growth dynamics were studied using the time-lapse image stacks. The viability of the single cells is 95.2% (N=23, see Table 2). The growth curves of 10 single cells are shown in Figure 3c. There was significant cell proliferation variance among even these 10 cells. The growth parameters, including time to attach on the well floor and to first divisions, and the population doubling time are listed in Table 2. Following single cell trapping, and flushing using DMEM with 30% FBS, 2% P-S and 50 µg/mL fibronectin to displace excessive cells, the trapped single cells required 4.83 (± 5.1) hours (N=12) to totally attach (before spreading) on the well bottom. It is well known that HDFs can quickly attach to the well plates and PDMS surfaces coated with fibronectin after seeding, so this delay in attachment is likely related to the presence of the BSA coating. On average, the single cells divided into two daughter cells in 42.7 (± 9.1) hours (N=10). The cell doubling time by Day 5 was 42.2 (± 11.3) hours (N=12).

Table 2. The single cell growth parameters

| Cell type | Viability | Attachment time (hours) | Time to first division (hours) | Doubling time (hours) |
|---|---|---|---|---|
| HDFs (Non-synchronised) | 95.2% | 4.83 ± 5.1 | 42.7 ± 9.1 | 42.2 ± 11.3 |
| HDFs (synchronised) | 94.3% | N/A | 77.5 ± 26.5 | 94.3 ± 40.4 |
| K562 | 91.1% | N/A | 24.1 ± 17.5 | 46 ± 5.3 |

The fluorescence and phase contrast images of two clones on Day 14 in separate wells are shown in Figure 3e and f. The cell morphology between these two clones is significantly different, while it is similar for the same clone. The surface area of cells in Figure 3e is much larger than that in Figure 3f, whilst the cells in Figure 3e are more elongated than those in Figure 3f.

The binary branching trees in Figure 3g indicate the individual cell pedigrees over five generations. The circles and the vertical lines represent the cells and generation time, respectively. A circle with a cross indicates cells moving out of the field of view. The proliferation of a single cell to multiple progeny and the relationship between the progeny can be clearly studied using the lineage tree. It was found that there was a delay of around 39 hours before the single cells started dividing. The generation time of progeny in the same clone varied from 14.5 to 39 hours. The mean generation time varies over a smaller range from the second generation (see Figure 3h). The mean (± standard deviation) generation time of these two clones is 21.3 (±7.1) hours (N=27).

The growth curves in Figure 3c and d and doubling times in Table 2 showed that the single synchronised cells (doubling time=94.3 hours, N=22) cultured in the microfluidic device grew much slower than the non-synchronised single cells (doubling time=42.2hours, N=12). The viability of the trapped synchronised single cells is 94.3% (N=26, see Table 2). The time to first division after single cell trapping is 79.4 ± 16.7 (N=26) hours. Although

Lab on a Chip Accepted Manuscript

Journal Name

RSCPublishing

ARTICLE

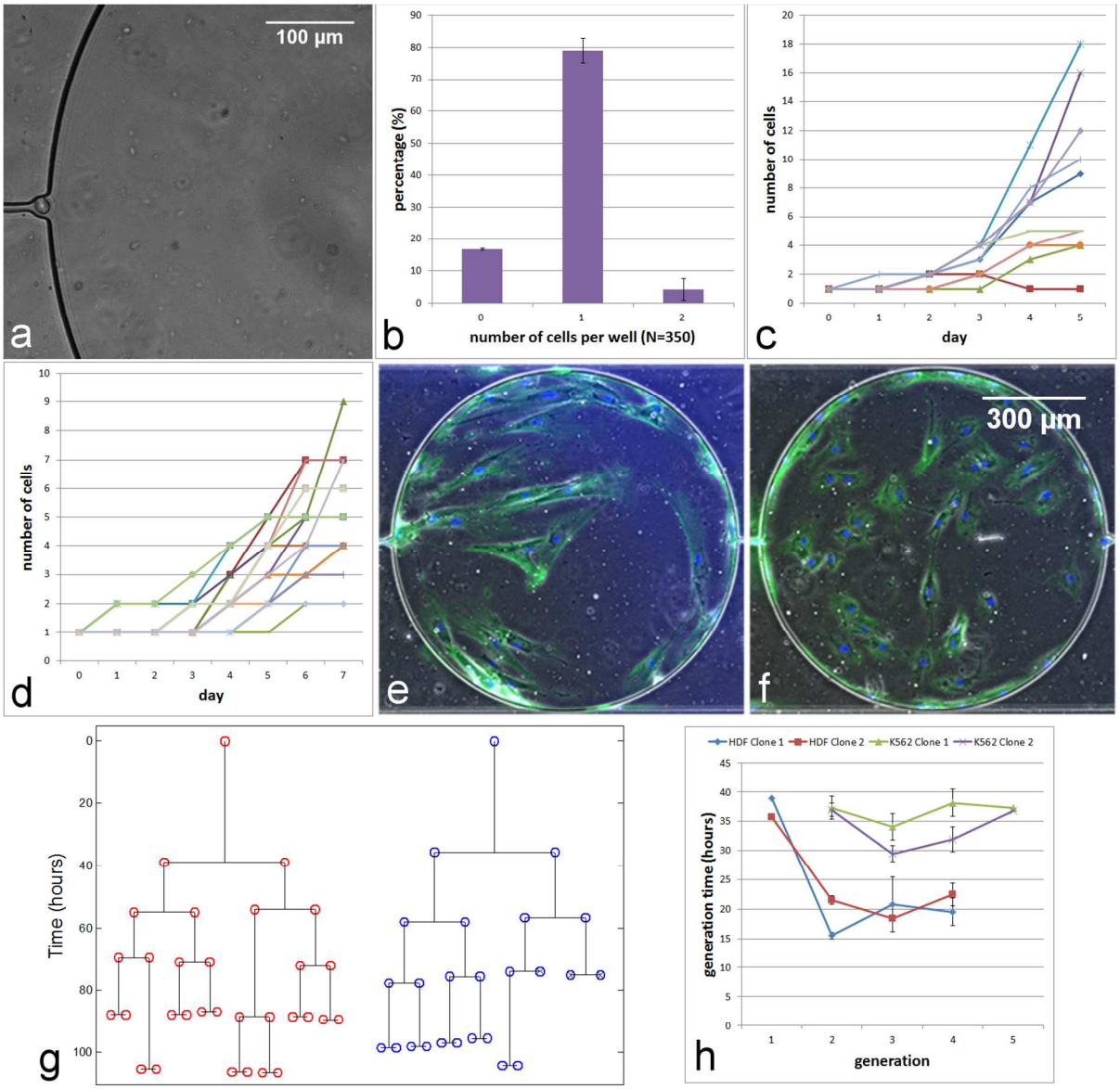


Figure 3. (a) The percentage of wells with 0, 1 and 2 cells (N=350). Error bars represent standard deviation. (b) The microphotograph of a single cell trapped in Device '1-27'. The growth curves of 10 non-synchronised HDF cells in 5 days (c) and 22 synchronised HDF cells in 7 days. e) and f) Two HDF clones with 47 (e) and 91 (f) progeny cells on Day 14 in two wells. (g) Lineage trees of two HDF cell clones. The circles and the vertical lines represent the cells and generation time, respectively. The circles with × indicate cells moving out of the field of view. (h) The variation of the mean (±standard error) generation time over 4 generations in the same clone of HDFs and K562 cells.

the cells were at G0/G1 phases when trapped, the time to first division still showed significant variance. There were 43.7% cells remaining in the non-divided state over the whole culture period. The growth curves of 22 synchronised cells are shown in Figure 3d. These obvious cell growth rate variations indicate that even when the cells have been synchronised to G0/G1 phases, cell growth heterogeneity is still evident.

### Single cell culture of non-adherent cells

The tree-pattern device (Design B in Figure 1b) can effectively trap single K562 cells with higher efficiency than that of single HDFs. 89.8% of wells (N=88) were seeded with single K562 cells. The mean diameter ± standard deviation of K562 cells cultured in flasks and trapped in the microdevice is 19.9 ± 2.5

Lab on a Chip Accepted Manuscript

μm (N=825, see Figure 4a, left) and 17.1 ± 1.6 μm (N=60, see Figure 4a, right), respectively. This trapped cell diameter is of a smaller range compared to the diameter range of normal growing cells. This indicates that the device is able to select the cells slightly smaller than the mean cell diameter.

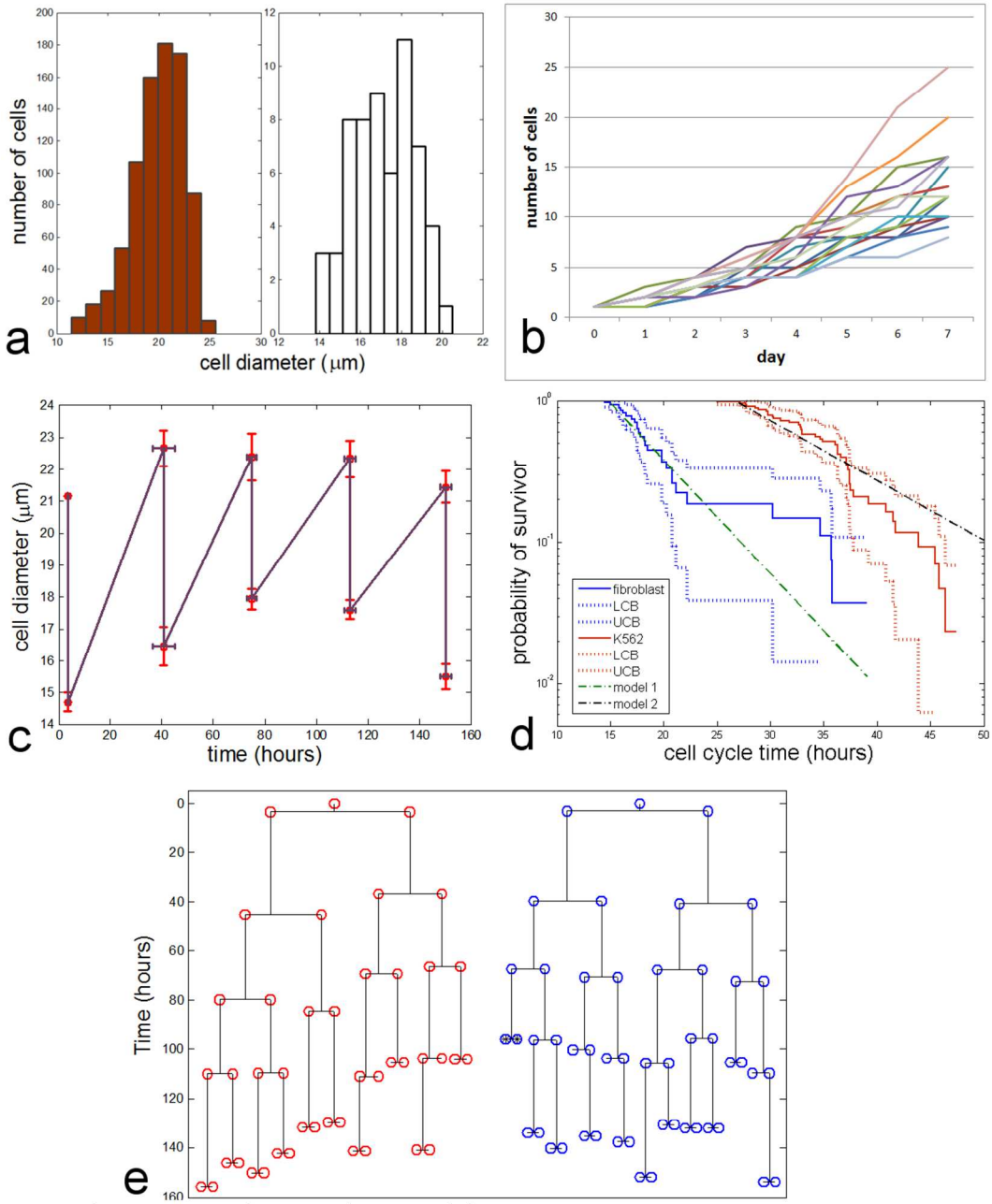


Figure 4. (a) The diameter of non-synchronised (bulk culture) K562 cells (left, N=825) and the single K562 cells (right, N=60) trapped in the tree-pattern device. (b) The growth curves of 16 single K562 cells in 7 days. (c) The cell size before and after cell division in multiple generations of the same clone. Horizontal error bars represent the standard error of mean for the cell division time and the vertical error bars indicate the standard error of mean of the cell diameter. Time at each vertical line is the time when the cells give birth to the next generation. (d) Empirical survivor (non-division) function of the cell cycle time for both HDFs (N=27) and K562 (N=43) cells. The solid lines are the cell cycle time. The dotted lines are the lower and upper confidence bounds. The dash-dot lines are the statistic models. (e) Lineage trees of two K562 clones. The circles with * indicate cell death.

The trapped single K562 cells and their progeny were stably retained in the wells and were not flushed out of the wells by the perfusion of the media during the 7-day culture period. All the cells were able to be continuously imaged to monitor their growth and division over 7 days. The viability of the trapped single cells during the long-term culture is 91.1% (N=72, see Table 2). The growth curves of 16 single cells were acquired from the time-lapse image stacks and are shown in Figure 4b. The mean time to the first division of the K562 cells after trapping is 24.1 (± 17.5) hours (N=72). The mean doubling time of the single cells shown in Figure 4b is 46 (± 5.3) hours (N=16). Two clones in separate wells were semi-automatically tracked for six generations. The lineage trees of both clones over 6 generations are shown in Figure 4e. The two mother

Lab on a Chip Accepted Manuscript

cells divided in 3.5 hours after trapping. This is a much smaller time than the generation time of the progeny, since the two mother cells were not newly born cells when they were trapped in the wells. The generation time of cells in K562 Clone 2 (see Figure 3h) varied from 27.2 to 46.4 hours. The mean generation time (± standard deviation) of two clones is 35.5 (±5.7) hours (N=43).

The cell sizes before (the top end of vertical lines) and after (the bottom end of vertical lines) cell division in multiple generations of the same clone are shown in Figure 4c. The time interval at each vertical line is the time over which the cells give birth to the next generation. Horizontal error bars represent the standard error of the mean for the cell division time and the vertical error bars indicate the standard error of the mean of the cell diameter. The cell size increases as the cell grows (DNA replication) and reaches the maximum value just before cell division. After division it gives birth to two smaller daughter cells. The maximum cell diameter before division was 21.9 (±1.7) μm (N=27), whereas the minimum cell diameter was 16.9 (±1.5) μm (N=37). The cell size increased by 30% from the stage of birth to the division. The cell sizes were not significantly different before division ($p=0.55$), while they were significantly different immediately after division ($p=1 \times 10^{-5}$).

## Discussion

### CFD analysis

The CFD study and the mechanical equilibrium analysis using the single-well model take into account of the cell-fluid interaction in the U-shaped hydrodynamic trap region and provide an computational economic method for single cell docking prediction [20]. It can be concluded from the CFD study that the fluid induced forces and the shear stress on the single cell are directly proportional to the Re (see Table S2 for the constants) when $0.0005 \leq Re \leq 1.8$. According to the mechanical equilibrium analysis (See Supplementary Material), one can conclude that the cell (either 14 μm or 24 μm in diameter) can be stably trapped in all models when $0.0005 \leq Re \leq 1.8$. The linear regression models and the mechanical equilibrium analysis predict the shear stress on the cell and hence guide the design of microfluidic devices. Compared to model 50-50, a deeper well with 50-μm high channel (model 50-250) only slightly reduced the fluid induced forces and torque on the cell (Figure S3e), while increasing the channel height to 100 μm results in significantly reduced drag, torque and shear stress on the cell (Figure S3 d and e). In model 50-50L, the larger cell (Ø 24 μm) is subjected to much larger drag and shear stress. To work out the critical Re when the cell was flushed out of the trap/well in model 50-50, the fluid induced forces at Re equal to 10, 11, 12, 15 and 20 were acquired from the CFD analysis. It is found that the trapped cell will not lift out of the well until the drag force becomes positive in the z direction (Figure S3f). The critical Re for the cell lifting out of the well in Model 50-50 is between 11 and 12. Therefore, in terms of the mechanical equilibrium analysis, the single cell trapping mechanism developed in this study is robust and reliable for a large Re range, which makes the process of single cell capture easy and repeatable.

### Single microsphere/cell trapping

The computational prediction for trapping was further confirmed by both the single microsphere and single cell trapping studies. For microspheres smaller than the width of the U-shaped trap (27 or 18 μm), while larger than the width of the notch channel (10 μm), high values of SSTE (97.5-98.5%) were observed when the Re varied, as shown in Figure 2.

The first advantage of the trapping mechanism is that once the microsphere/cell is trapped in the U-shaped trap, it remains fixed and can withstand variations in flow rate (Re) to a large extent. For example, the SSTE remains around 98.5% when Re increases from 0.2 to 1.8. This confirmed the prediction from the equilibrium analysis from CFD of a single cell within a trap. The large Re range applicable to single cell/microsphere trapping confirms that this design offers great flexibility and reliability for the single cell trapping process. In other words, after the manual loading of cells into the device, the Re for media injection does not require accurate levels of fluid control, making the operation of the device easy and simple.

The second advantage of the trapping mechanism is its ability to select the microsphere/cell based on size. If we assume that the width of the trap and the notched channel is $W_{trap}$ and $W_{channel}$, respectively and the diameter of microspheres / cells is $D$. When $D < W_{channel}$, microspheres/cells are able to freely flow through the trap. While when $D > W_{trap}$, microspheres / cells may be easily displaced out of the trap at even low flushing flow rates (see Figure 2d). Therefore, the device can selectively trap microspheres/cells with the diameter $D$ ( $W_{channel} < D < W_{trap}$ ) through simply controlling the flushing flow rate.

The third advantage of this trapping mechanism is high throughput and the rapid trapping of hundreds / thousands of single cells in a few minutes at the flow rate of 0.5 μL/min. This short trapping period and small flushing flow rate are extremely important for shear sensitive cells [34], since they minimise the exposure of cells to fluid shear stress and the risk of undesired differentiation of stem cells due to shear stress [35].

One critical requirement for trapping single cells, as predicated by the CFD study, is keeping cells spherical and non-adhered to the surface during the cell trapping process. Carlo et al. reported that to successfully trap HeLa cells in a PDMS based microfluidic device, they were resuspended in PBS and loaded into the device within 15 min following the trypsinisation [22]. However, fibroblast cells are extremely adhesive and able to immediately bind to the untreated PDMS surface following cell loading and hence cannot be trapped as suspended single cells. BSA has been extensively employed as a substrate coating to prevent undesired cell adhesion. In this study we confirmed that the application of a solution of 0.8% BSA (in PBS) to coat the PDMS surface was sufficient to prevent the non-specific cell adhesion of HDFs for a few minutes whilst single cells were trapped.

Lab on a Chip Accepted Manuscript

 This journal is © The Royal Society of Chemistry 2012

Compared to the single microsphere trapping efficiency (98.2%) of 25 µm microspheres in the Device '1-27', the single HDF cell trapping efficiency in the serpentine device (Design A) is lower - 79.5% of the traps (N=350) are loaded with single HDFs. In addition, if the flush flow rate was as high (Re>0.2) as that in the single microsphere trapping experiment, significantly lower numbers of single cells will be trapped. This trapping efficiency difference is related to the rigidity difference between microspheres and cells. The microspheres are rigid and not able to be deformed even at high flow rates and they can be stably trapped in situ, as predicted by the CFD model. However, cells are flexible and hence deform significantly at even low flow fluid shear stress, and therefore they are subject to different drag forces, which cause the lifting up of cells from the single cell trap. Thankfully, reducing the flush flow rate enables one to effectively increase the single cell trapping efficiency.

The trapping of single non-adherent cells in the tree-pattern device (Design B in Figure 1b) as used herein was shown to be much easier than that for the adherent cells, since non-adherent cells are not adhesive to the PDMS surface. The capture process of the non-adherent cells can thus be predicted using the rigid sphere model (see S1.2 in Supplementary Materials), and the deposition process completed in a few minutes. The single cell trapping efficiency of K562 cells is 89.8%. It is higher than that of HDFs (79.5%) due to their size difference. The deformability of K562 cells compared to the microspheres likely contributes to the slightly lower single cell trapping efficiency than that of single microspheres (98.5%). The size range of trapped single K562 cells is smaller than that of K562 cells cultured in flasks. This confirms the size selection capability of the design. If the trap size and the width of the microchannel connecting two wells are appropriately specified, this design can be applied for selectively trapping and long-term culture of cells of desired size.

**Single cell culture**

Following the high-throughput single cell trapping, both HDFs (both synchronised and non-synchronised) and K562 cells were cultured in situ with media perfusion and time-lapse imaging for at least a week. The 50 µg/mL fibronectin added into the HDF culture media was able to promote the cell adhesion on the BSA coated surface. This study further shows that post this surface modification step, trapped single HDFs may adhere to and spread on the bottom of the trap, and gradually migrate into the well. The well provides enough surface area for the trapped cells (especially the HDFs with large surface area) and their progeny to grow. The migration of most progeny was successfully confined in the same well and hence enabled the continuous imaging over extended periods of time. In the case of tree-pattern device (Design B), the introduction of the tree-pattern channel splitting the media flow into 32 channels effectively reduces the shear stress imposed on the cultured K562 cells. The small Reynolds number flows are not able to flush the cells and progeny out of the wells, enabling the continuous imaging of all progeny in the same field of view.

The growth curves of both HDF and K562 cells reveal that there is substantial growth heterogeneity at the single cell level. Importantly, the variation in the growth rates of HDFs synchronised in the G0/G1 phase indicates that the observed growth heterogeneity within cell populations is inherent to the nature of individual cells rather than an influence of the status of the cell cycle at cell seeding. The time to first division and population doubling time for non-synchronised HDFs, synchronised HDFs and K562 cells are summarised in Table 2. The population doubling time of single non-synchronised HDFs and K562 cells in this study is 42.2 ± 11.3 and 46 ± 5.3 hours, respectively. They are larger than the reported doubling times of 25.4 hours for HDFs [36] and 24 hours for K562 cells [37] when cultured in populations. From the lineage tree of two HDF clones (see Figure 3g), it is found that first generation time is longer than the mean generation time. This is likely due to the fact that the trapped single cells (mother cells) have to firstly adhere (taking 4.83 hours, N=12) and spread on the surface of the well (requiring protein synthesis and reorganisation of the cytoskeleton) prior to progressing into mitosis, whilst the daughter cells were observed to be able to adhere to the surface immediately after this division event. In stark contrast, there is no delay of the first division for the non-adherent K562 cells (see Figure 4e). This indicates that for the K562 cells, i) the mother cells were at G3/M phases and were about to divide during cell seeding and ii) the non-adherent cells do not need time to adapt to the microenvironment and are able to grow immediately following trapping.

The cell growth/division data from single cell starting point shown in Figures 3 and 4 can be further analysed using the cell lifetime. Kaplan-Meier statistics were applied to determine the empiric survival (no-division) of the cells using the cell cycle time of the HDF (Figure 3g) and K562 (Figure 4e) clones. The probability of survival (±95% confidence bounds) is shown in Figure 4d. The generation time distribution was studied using the Smith-Martin model [21, 38]. The probability (*Pr*) of non-division (survival) of a cell at the specific cell age T is given by:

$$Pr[T > t] = \exp[-\lambda(t - \tau_0)]$$

The cell cycle parameters (see Table 3) in the Smith-Martin model were acquired using linear regression analysis of the probability of the survivor. $\tau_0$ is the time lag (obligate period of time) for the cell to replicate DNA before division. The cell cycle time ($\tau_0 + \lambda^{-1}$) acquired from the model is similar to the observed cell cycle time as shown in Table 3.

Lab on a Chip Accepted Manuscript

Table 3. The cell cycle parameters of the Smith-Martin model

| Cells | $\lambda$ | $\tau_0$ | Cell cycle time (hours) from the model $(\tau_0 + \lambda^{-1})$ | Observed cell cycle time (hours) |
|---|---|---|---|---|
| HDFs | 0.1851±0.0233 | 14.76±0.3 | 20.2 | 21.3 |
| K562 | 0.09741±0.0128 | 26.65±0.69 | 36.9 | 35.3 |

## Conclusions

This paper details the design, fabrication and validation of a microfluidic device with the capacity to incorporate hundreds to thousands of culture wells that include a U-shaped hydrodynamic micro-trap with a notched microchannel on the downstream edge of each well. This device enables quick, high-throughput, deterministic single cell trapping and *in-situ* culture of both adherent and non-adherent cells for extended periods of time with media perfusion and continuous time-lapse imaging. Size selectivity of the hydrodynamic trap was confirmed using both microspheres and somatic cells. The maximum tapping efficiency of single microspheres, HDF and K562 cells is 98.5%, 78.9% and 89.8%, respectively. Both single adherent HDFs and non-adherent K562 cells were successfully trapped and cultured in hundreds to thousands of wells with continuous time-lapse imaging for a period of 7 days. It is found that the population doubling time of both single HDF and K562 cells are larger than those cultured as bulk populations in static plates. Elementary clonal analysis of both somatic cell types with and without cell cycle synchronisation reveals that the observed growth heterogeneity of single somatic cells is an inherent property of the individual cells, and not a result of the distribution of cells in different cell cycle status. This validated device platform is simple to fabricate and to use, and permits long-term culture from single cell starting points, and is expected to find applications in multiple fields of research, including stem cells, cellular therapies and regenerative medicine.

## Acknowledgements

The authors would like to acknowledge the financial support provided by the Australian Research Council Special Research Initiative Scheme (Stem Cells Australia, SRI110001002). The authors would also like to acknowledge Vincent Trachsel for drawing Figure 1c, and Prof. Lars Nielsen for providing the K562 cells. This work was performed in part at the Queensland node of the Australian National Fabrication Facility (ANFF), a company established under the National Collaborative Research Infrastructure Strategy to provide nano and microfabrication facilities for Australian researchers. The CFD analysis was performed using facilities at the High-Performance Computing cluster, The University of Queensland.

## Notes and references

a Tissue Engineering and Microfluidics Laboratory, Australian Institute for Bioengineering & Nanotechnology, The University of Queensland, St. Lucia, QLD 4072, AUSTRALIA.
b Stem Cell Engineering Laboratory, Australian Institute for Bioengineering & Nanotechnology, The University of Queensland, St. Lucia, QLD 4072, AUSTRALIA.
c School of Chemical Engineering, The University of Queensland, St. Lucia, QLD 4072, AUSTRALIA.
d Materials Science and Engineering Division, CSIRO, Clayton, VIC 3169, AUSTRALIA.
* Correspondence: Professor Justin J. Cooper-White, Email: j.cooperwhite@uq.edu.au.

Electronic Supplementary Information (ESI) available: [details of any supplementary information available should be included here]. See DOI: 10.1039/b000000x/

## References

1. V. Lecault, M. VanInsberghe, S. Sekulovic, D. Knapp, S. Wohrer, W. Bowden, F. Viel, T. McLaughlin, A. Jarandehei, M. Miller, D. Falconnet, A. K. White, D. G. Kent, M. R. Copley, F. Taghipour, C. J. Eaves, R. K. Humphries, J. M. Piret and C. L. Hansen, *Nature Methods*, 2011, 8, 581-U593.
2. S. L. Faley, M. Copland, D. Wlodkowic, W. Kolch, K. T. Seale, J. P. Wikswo and J. M. Cooper, *Lab on a Chip*, 2009, 9, 2659-2664.
3. T. Graf and M. Stadtfeld, *Cell Stem Cell*, 2008, 3, 480-483.
4. J. Shu, C. Wu, Y. Wu, Z. Li, S. Shao, W. Zhao, X. Tang, H. Yang, L. Shen, X. Zuo, W. Yang, Y. Shi, X. Chi, H. Zhang, G. Gao, Y. Shu, K. Yuan, W. He, C. Tang, Y. Zhao and H. Deng, *Cell*, 2013, 153, 963-975.
5. H. A. Svahn and A. van den Berg, *Lab on a Chip*, 2007, 7, 544-546.
6. D. M. Titmarsh, H. Chen, E. J. Wolvetang and J. J. Cooper-White, *Biotechnology Journal*, 2012, DOI: 10.1002/biot.201200149, n/a-n/a.
7. H. Chen and R. Nordon, in *Emerging Trends in Cell and Gene Therapy*, eds. M. K. Danquah and R. I. Mahato, Humana Press, 2013, DOI: 10.1007/978-1-62703-417-3_19, ch. 19, pp. 435-470.
8. D. Titmarsh, A. Hidalgo, J. Turner, E. Wolvetang and J. Cooper-White, *Biotechnology and Bioengineering*, 2011, 108, 2894-2904.
9. P. J. Hung, P. J. Lee, P. Sabounchi, R. Lin and L. P. Lee, *Biotechnology and Bioengineering*, 2005, 89, 1-8.
10. L. Kim, Y. C. Toh, J. Voldman and H. Yu, *Lab Chip*, 2007, 7, 681-694.
11. G. Roman, Y. Chen, P. Viberg, A. Culbertson and C. Culbertson, *Analytical and Bioanalytical Chemistry*, 2007, 387, 9-12.
12. B. Huang, H. Wu, D. Bhaya, A. Grossman, S. Granier, B. K. Kobilka and R. N. Zare, *Science*, 2007, 315, 81-84.
13. R. Gomez-Sjoberg, A. A. Leyrat, D. M. Pirone, C. S. Chen and S. R. Quake, *Anal. Chem.*, 2007, 79, 8557-8563.
14. L. Chau, M. Doran and J. Cooper-White, *Lab Chip*, 2009, 9, 1897-1902.
15. H. Chen, J. Cornwell, H. Zhang, T. Lim, R. Resurreccion, T. Port, G. Rosengarten and R. E. Nordon, *Lab on a Chip*, 2013, DOI: 10.1039/c3lc50123j.
16. L. G. Vincent, Y. S. Choi, B. Alonso-Latorre, J. C. del Alamo and A. J. Engler, *Biotechnology Journal*, 2013, 8, 472-+.

Lab on a Chip Accepted Manuscript

 This journal is © The Royal Society of Chemistry 2012

17. D. M. Titmarsh, J. E. Hudson, A. Hidalgo, A. G. Elefanty, E. G. Stanley, E. J. Wolvetang and J. J. Cooper-White, *Plos One*, 2012, 7, e52405-e52405.
18. S. Sugiura, K. Hattori and T. Kanamori, *Analytical Chemistry*, 2010, 82, 8278-8282.
19. M. C. Park, J. Y. Hur, H. S. Cho, S. H. Park and K. Y. Suh, *Lab Chip*, 2011, 11, 79-86.
20. H. Chen, G. Rosengarten, M. Li and R. E. Nordon, *Journal of Micromechanics and Microengineering*, 2012, 22.
21. H. Chen, J. Li, H. Zhang, M. Li, G. Rosengarten and R. E. Nordon, *Biomicrofluidics*, 2011, 5, 044117-044113.
22. D. D. Carlo, L. Y. Wu and L. P. Lee, *Lab on a Chip*, 2006, 6, 1445-1449.
23. A. Lawrenz, F. Nason and J. J. Cooper-White, *Biomicrofluidics*, 2012, 6.
24. S. Kobel, A. Valero, J. Latt, P. Renaud and M. Lutolf, *Lab on a Chip*, 2010, 10, 857-863.
25. M. C. Shannon L. Faley, Donald Wlodkowic, Walter Kolch, Kevin T. Seale, John P. Wikswo and Jonathan M. Cooper, *Lab Chip*, 2009, 9, 6.
26. L. Y. Lin, Y. S. Chu, J. P. Thiery, C. T. Lim and I. Rodriguez, *Lab on a Chip*, 2013, 13, 714-721.
27. C. Yan, J. Sun and J. Ding, *Biomaterials*, 2011, 32, 3931-3938.
28. J. R. Rettig and A. Folch, *Anal. Chem.*, 2005, 77, 5628-5634.
29. D. Di Carlo, L. Y. Wu and L. P. Lee, *Lab Chip*, 2006, 6, 1445-1449.
30. J.-P. Frimat, M. Becker, Y.-Y. Chiang, U. Marggraf, D. Janasek, J. G. Hengstler, J. Franzke and J. West, *Lab on a Chip*, 2011, 11, 231-237.
31. D. Titmarsh and J. Cooper-White, *Biotechnology and Bioengineering*, 2009, 104, 1240-1244.
32. H. Y. Chen, G. Rosengarten, M. S. Li and R. E. Nordon, *Journal of Micromechanics and Microengineering*, 2012, 22.
33. M. Chen, J. Huang, X. Yang, B. Liu, W. Zhang, L. Huang, F. Deng, J. Ma, Y. Bai, R. Lu, B. Huang, Q. Gao, Y. Zhuo and J. Ge, *Plos One*, 2012, 7.
34. Y. C. Toh and J. Voldman, *Faseb Journal*, 2011, 25, 1208-1217.
35. G. Yourek, S. M. McCormick, J. J. Mao and G. C. Reilly, *Regenerative Medicine*, 2010, 5, 713-724.
36. M. B. Ruffy, S. S. Kunnavatana and R. J. Koch, *Archives of Facial Plastic Surgery*, 2006, 8, 329-332.
37. T. Rutherford, J. B. Clegg, D. R. Higgs, R. W. Jones, J. Thompson and D. J. Weatherall, *Proceedings of the National Academy of Sciences of the United States of America-Biological Sciences*, 1981, 78, 348-352.
38. R. E. Nordon, K.-H. Ko, R. Odell and T. Schroeder, *Journal of Theoretical Biology*, 2011, 277, 7-18.

Lab on a Chip Accepted Manuscript